Int J Earth Sci (Geol Rundsch) (2012) 101:339–349
DOI 10.1007/s00531-011-0658-y

ORIGINAL PAPER

Time calibration of sedimentary sections based on insolation cycles using combined cross-correlation: dating the gone Badenian stratotype (Middle Miocene, Paratethys, Vienna Basin, Austria) as an example

Johann Hohenegger · Michael Wagreich

Received: 31 August 2010 / Accepted: 4 April 2011 / Published online: 19 April 2011

Abstract Cross-correlation between insolation intensities and a combination of sedimentary characters is introduced to obtain precise time calibration of sedimentary cycles. The first step is to transfer the section scale into ages using power spectra comparing the main periods with orbital cycles, while in the second step the standardized values of sedimentary signals are cross-correlated with the standardized insolation curve. As an example for the applicability of the method, we investigated calcium carbonate, organic carbon in a 9-m sampled section from the historical Badenian stratotype at Baden/Sooss (Lower Austria). Comparing courses of geochemical parameters between the historical stratotype and a nearby drilled 102-m scientific core resulted in continuation of the core section into the stratotype. Cross-correlation between magnetic susceptibility (MS) combined with the negatively correlated calcium carbonate content of the drilled section on the one side and summer solar insolation at 65° northern latitude on the other resulted in an extremely significant correlation between −14.221 and −13.982 Ma. This is younger than the before estimated time frame (−14.379 to −14.142 Ma) based on cross-correlation between MS and the orbital 100-kyr eccentricity and 41-kyr obliquity cycles. The direct continuation of the drilled section by the stratotype covering a time span of 17.7 kyr consequently dates the Badenian stratotype between −13.982 and −13.964 Ma. Therefore, the upper limit of the stratotype, assigned to the Early Badenian, puts it close to the Langhian/Seravallian boundary at −13.82 Ma, demonstrating the need for revising the Badenian stratigraphic subdivision based on orbital cycles, especially the middle Badenian Wielician substage.

Keywords Cross-correlation · Insolation · Geochemical parameters · Badenian · Miocene

J. Hohenegger (✉)
Department of Palaeontology, University of Vienna,
1090, Vienna, Austria
e-mail: johann.hohenegger@univie.ac.at

M. Wagreich
Department of Geodynamics and Sedimentology,
Center for Earth Sciences, University of Vienna,
1090, Vienna, Austria

Introduction

Absolute dating of deep-time stratigraphic intervals and their representative sedimentary sections poses a major problem. Achievements in timescales and improvements in dating methods expand precise absolute age dating into increasingly older stratigraphic horizons, based on more and more precise absolute rock and mineral dating methods and the application of orbital timescales. Especially for the Neogene period, a continuously improving timescale is available (Lourens et al. 2004) and orbital tuning of the record of marginal seas like the Paratethyan is in progress (e.g., Hohenegger et al. 2009a, b, c; Lirer et al. 2009; Sprovieri et al. 2003).

This paper presents the unique case of age dating solely by insolation intensities for a stratotype that is not accessible anymore at the moment. The Badenian stage comprises a regional Central Paratethyan stage which is of early Middle Miocene Age and which was suggested to be correlated, at least in parts, to the Langhian stage (Rögl et al. 2002). However, a detailed correlation to the scale ATNTS2004 (Lourens et al. 2004) is hindered by reduced oceanic connections of the Paratethyan Sea, and several solutions were suggested for this stratigraphic problem

(e.g., Kocsis et al. 2009; Piller et al. 2007). Precise correlations are furthermore hindered by the fact that the Badenian stratotype section, as defined by Papp and Steininger (1978) in the Vienna Basin, is now covered and inaccessible. By chemostratigraphic cycles recognized in a sample set taken in the 1980s and in combination with chemical and magnetostratigraphic data from a nearby scientific borehole (Hohenegger et al. 2008), we are able to precisely correlate the Badenian stratotype to the global orbital timescale and thus to date the stratotype of the Badenian for the first time precisely.

Geological setting and stratigraphy

The Badenian comprises a stage of the regional Paratethyan stratigraphical scheme (Cicha et al. 1975; Papp et al. 1968). Its history of definition dates back to the first half of the Nineteenth Century (e.g., Keferstein 1828), and the stage was and is used widely in the Central Paratethys. Recent overviews and regional analysis of the Paratethys, including the Badenian, are given by Harzhauser and Piller (2007), Kováč et al. (2004), and Piller et al. (2007). The Paratethys Sea was a remnant of the vanishing Tethys during Cenozoic Africa/Eurasia collision and Alpine mountain building (e.g., Popov et al. 2004). Due to its separate biogeographic evolution, regional chronostratigraphic/geochronologic scales were established.

The Badenian stratotype section was defined by Papp and Steininger (1978) in the old brick yard Baden/Sooss near the town Baden (Lower Austria), south of Vienna. The stratotype section is situated in the southern part of the Vienna Basin, near its western margin (Fig. 1). The stratotype is now used as a waste dump and is totally covered by waste material, except a very small and strongly weathered 1.5-m ditch, and a small area preserved as a natural monument (Rögl et al. 2008).

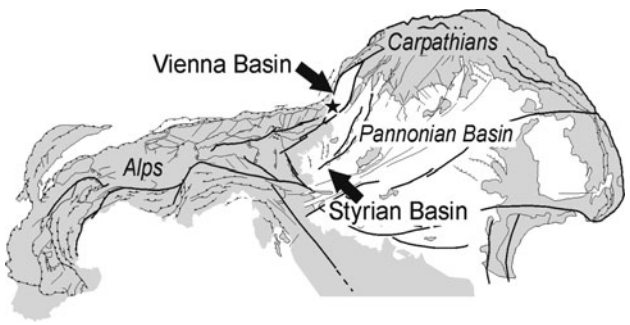

Fig. 1 Overview map of the Alps and Carpathians with the Vienna Basin and the Styrian Basin. *Star* indicates position of the Badenian stratotype near Baden/Sooss in the southern Vienna Basin

To investigate the stratigraphy in that area, a scientific core was taken near the former outcrop which sampled a 100-m section structurally below the stratotype (geographic coordinates WGS84: E016°13′44″, N47°59′24″). This core section, which completely belongs to the (local) Upper Lagenidae Zone, was investigated for stratigraphy, paleoecology, paleoenvironments, and cyclicity (see Hohenegger et al. 2008, 2009a, b, and references therein). The lower, tectonically undisturbed section part of the Baden/Sooss core was dated by orbital cycles (Hohenegger et al. 2009a) using cross-correlation of cycles in magnetic susceptibility (Selge 2005), calcium carbonate, and organic carbon (Wagreich et al. 2008). The 44.9- and 22.5-m periods resulting from the decomposition of the highly correlated periodic functions in MS, $CaCO_3$, and organic carbon were equated with the 100-kyr eccentricity and the 41-kyr obliquity orbital cycles (Hohenegger et al. 2009a). The highest correlation between the orbital cycles and the corresponding largest sinusoidal waves of the section by transferring periods from meters into kyrs was found in the interval between -14.379 ± 0.001 and -14.258 ± 0.001 Ma. According to the resulting time interval of 121 kyr for this part of the section, the mean sedimentation rate was calculated as 512 mm kyr^{-1}. Adding the tectonically disturbed upper section, where calculations were only based on MS, the complete core section was dated from -14.379 to -14.142 Ma (Hohenegger et al. 2009a).

By combining those data with new data obtained from a sample set taken at the Badenian stratotype in the 1990s before the brick yard was used as a waste dump together with additional detailed investigation of $CaCO_3$ and organic carbon in the tectonically disturbed upper section of the drill, we are able to redefine the time calibration of the complete section core and to correlate the historical stratotype with the orbital timescale.

Time calibration method

Magnetic susceptibility (MS) was measured in 5 cm distances along the cored section (1,797 measurements), while $CaCO_3$ and organic carbon measured in 20 cm distances resulted in 475 measurements in each case. In samples from the additional 9-m section of the historical stratotype, only $CaCO_3$ and organic carbon could be measured, where sampling in 20 cm distances resulted in 43 measurements for each component.

Smoothing of the strongly oscillating functions was done by moving averages, where the interval lengths were 50 cm (11 measurements) in case of MS and 80 cm (5 measurements) for both chemical variables (Fig. 2). For the applicability of linear statistical methods, percentages

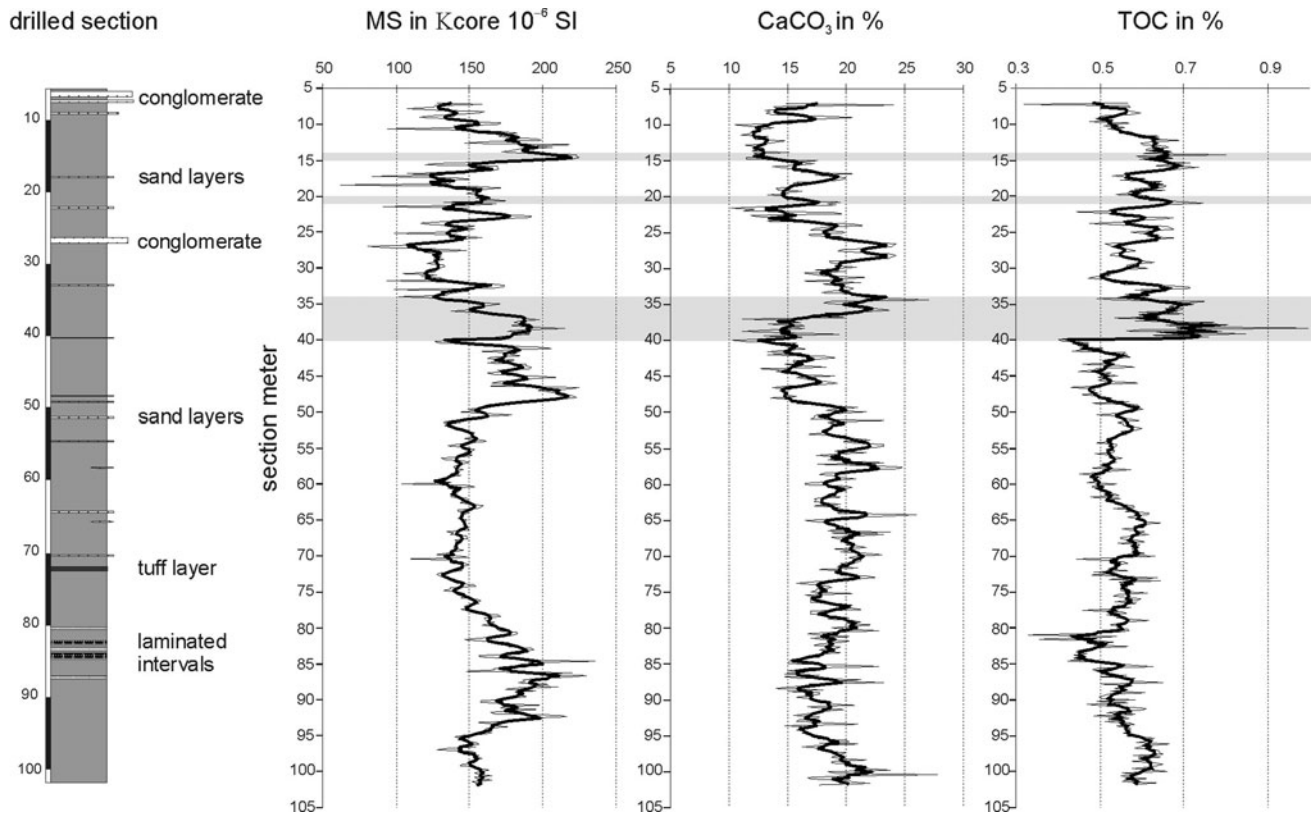

Fig. 2 Courses of magnetic susceptibility, calcium carbonate, and organic carbon measured in 20 cm distances along the drilled section; *thick black lines* indicate smoothing using interval length of 5 measurements. The *shaded areas* demonstrate strong environmental changes according to foraminiferal and nannoplankton composition

of calcium carbonate and organic carbon have been transformed into linear variables using the logit transformation (Linde and Berchtold 1976).

Each of the three oscillating functions (MS, $CaCO_3$, and C_{org}) could be fitted by the sinusoidal regression

$$y = M + \sum_{j=1}^{m} \left[A_j \cos\left(2\pi x/L_j - x_{0j}\right)\right]$$

where M represents the mean level, A the amplitude, L the period, and x_0 the acrophase of the jth component (Batschelet 1981). Period lengths L were obtained by power spectra analyses (Hammer and Harper 2006), and the remaining parameters were estimated by nonlinear regression. The transfer of section meters into time was done by regression between ages in kyr and the main period lengths obtained by power spectra analyses (Hohenegger et al. 2009a).

Cross-correlation (e.g., Davis 2002) was used to determine the best position of section parts along the timescale and section meters, respectively. The lag distance in cross-correlation was 20 cm in case of section meters and 1 kyr using time. When several variables were cross-correlated with solar insolation or orbital cycles, all variables had to be standardized to prevent weighting by scale differences.

Results

Time calibration of the section was checked by cross-correlation of oscillations in summer insolation intensity at 65° northern latitude (Laskar et al. 2004) with oscillations in MS and $CaCO_3$, whereby the latter got negative values due to its negative correlation with MS (Table 1). Since correlations between organic carbon on the one side and MS and calcium carbonate on the other change in the upper section from negative to positive correlations and vice versa (Table 1), C_{org} was excluded from cross-correlation. The tested time segment ranges from −14.500 to −13.800 Ma, based on available biostratigraphic constraints (Hohenegger et al. 2008, 2009a).

Transformation of section meters into time

For transferring section meters into time, periods of oscillating functions in MS, $CaCO_3$, and organic carbon were separately compared in the upper (7–38.8 m) and the lower section part (40–102 m) using power spectra analysis (Fig. 3). Afterward, the significant period lengths of the stratotype were compared with periods of both section parts.

Table 1 Correlations between of magnetic susceptibility, calcium carbonate, and organic carbon in both drill sections, based on the one side on samples and on the other on time transformed (kyrs) values

Lower section (40–102 m)			Upper section (7–40 m)		
Samples in 20 cm distance			Samples in 20 cm distance		
$n = 310$	MS	CaCO3	$n = 165$	MS	CaCO3
CaCO3	−0.636		CaCO3	−0.646	
$p(H_0)$	0.000		$p(H_0)$	0.000	
TOC	−0.321	0.440	TOC	0.605	−0.111
$p(H_0)$	0.000	0.000	$p(H_0)$	0.000	0.079
Samples in kyr distance			Samples in kyr distance		
$n = 124$	MS	CaCO3	$n = 111$	MS	CaCO3
CaCO3	−0.630		CaCO3	−0.656	
$p(H_0)$	0.000		$p(H_0)$	0.000	
TOC	−0.307	0.447	TOC	0.610	−0.120
$p(H_0)$	0.000	0.000	$p(H_0)$	0.000	0.105

In the lower section part (40–102 m), the MS is highly negatively correlated with $CaCO_3$ and less, but still negatively correlated with organic carbon leading to a significant positive correlation between both geochemical parameters (Table 1). Except the first period with a significantly shorter value for organic carbon (35.3 m) compared with the corresponding periods in MS (45.1 m) and calcium carbonate (44.9 m), there is strong coincidence in the following three periods for all variables (Fig. 3). When the averaged periods of 41.78, 21.87, 15.16, and 11.09 m obtained by regression analyses are related to the 100-kyr eccentricity, 41-kyr obliquity and both 23- and 19-kyr precession cycles (Hohenegger et al. 2009a), this leads to a time range of 123.2 kyr for the 61.8-m-long section inferring a sedimentation rate of 502 mm kyr^{-1}.

In the tectonically disturbed upper section part (7–38.8 m), the correlation between the three geophysical and geochemical variables changes significantly. While the negative correlation between MS and $CaCO_3$ is still high and of similar intensity as in the lower part, the correlation between MS and organic carbon switches from a negative correlation in the lower to a significant high positive correlation in the upper section part, while the correlation between both geochemical variables becomes insignificant (Table 1).

Periods between the three parameters do not correlate as well as in the lower section (Fig. 3); nevertheless, the period lengths of 29.50, 12.02, 8.18, and 5.84 m again can be correlated with the above-mentioned orbital cycles (100, 41, 23, and 19 kyr), leading to an equalization of the 33-m-long upper section with a time range of 110.4 kyr. Since there are no differences in sediments between the upper and the lower section part indicating no major differences in sedimentation rate, approximately 45% of the sediment is lost in the upper section due to post-depositional tectonics (Hohenegger et al. 2009a). Because the fault planes are randomly distributed along the upper section (Wagreich et al. 2008) as tested by Poisson distribution, the sedimentary gaps shorten the frequency curves more or less constantly preventing stronger distortion. Significant gaps due to tectonics according to abrupt environmental changes as indicated by benthic foraminifera and calcareous nannoplankton can be detected between section meters 14/15 and 21/22 (Ćorić and Hohenegger 2008). Additionally, the most significant gap between 34 and 41 m interrupting the continuous sedimentation is documented in oscillations of MS and $CaCO_3$, but extremely in the stepwise abrupt change in percentages of organic carbon (Fig. 2).

In the stratotype section, a single significant period is represented in the power spectra of both geochemical variables with 8.40 m ($CaCO_3$) and 9.60 m (organic carbon) lengths (Fig. 3). Correlating the mean of 9.00 m with the 19-kyr precession cycle, according to the relation between the period length of 11.09 m with the 19-kyr precession cycle in the undisturbed lower part of the drill section, results in a time correspondence of 17.7 kyr for the 8.4-m-long section. Since the stratotype showed undisturbed sedimentation (Papp and Steininger 1978), a sedimentation rate of 475 mm kyr^{-1} can be calculated for this part.

Dating the lower section part

This is the target section for basic dating because of the undisturbed and continuous sedimentation with more or less constant sedimentation rates. Calibrating the lower section part by cross-correlation between insolation on the one side and MS combined with the negative values for $CaCO_3$ on the other, 6 intervals within the time segment from −14.500 to −13.830 Ma demonstrate significant cross-correlations of 1% error probability (Fig. 4a).

According to the absence of the calcareous nannoplankton index fossil *Helicosphaera waltrans* with LCO (Last Common Occurrence) at −14.357 Ma (Abdul Aziz et al. 2008), the earliest significant interval from −14.460 to −14.336 Ma is improbable. The next two significant intervals from −14.299 to −14.176 Ma and −14.258 to −14.135 Ma are close to the $^{40}Ar/^{39}Ar$ dating as obtained for the middle part of the Lower Lagenidae Zone in the nearby Styrian Basin (Fig. 1) with −14.2 ± 0.1 Ma (Bojar et al. 2004) and −14.206 ± 0.066 Ma (biotite) versus −14.39 ± 0.12 Ma (sanidine) by Handler et al. (2006). The latter dating seems to be the better estimate according to the usage of sanidine and including reported time

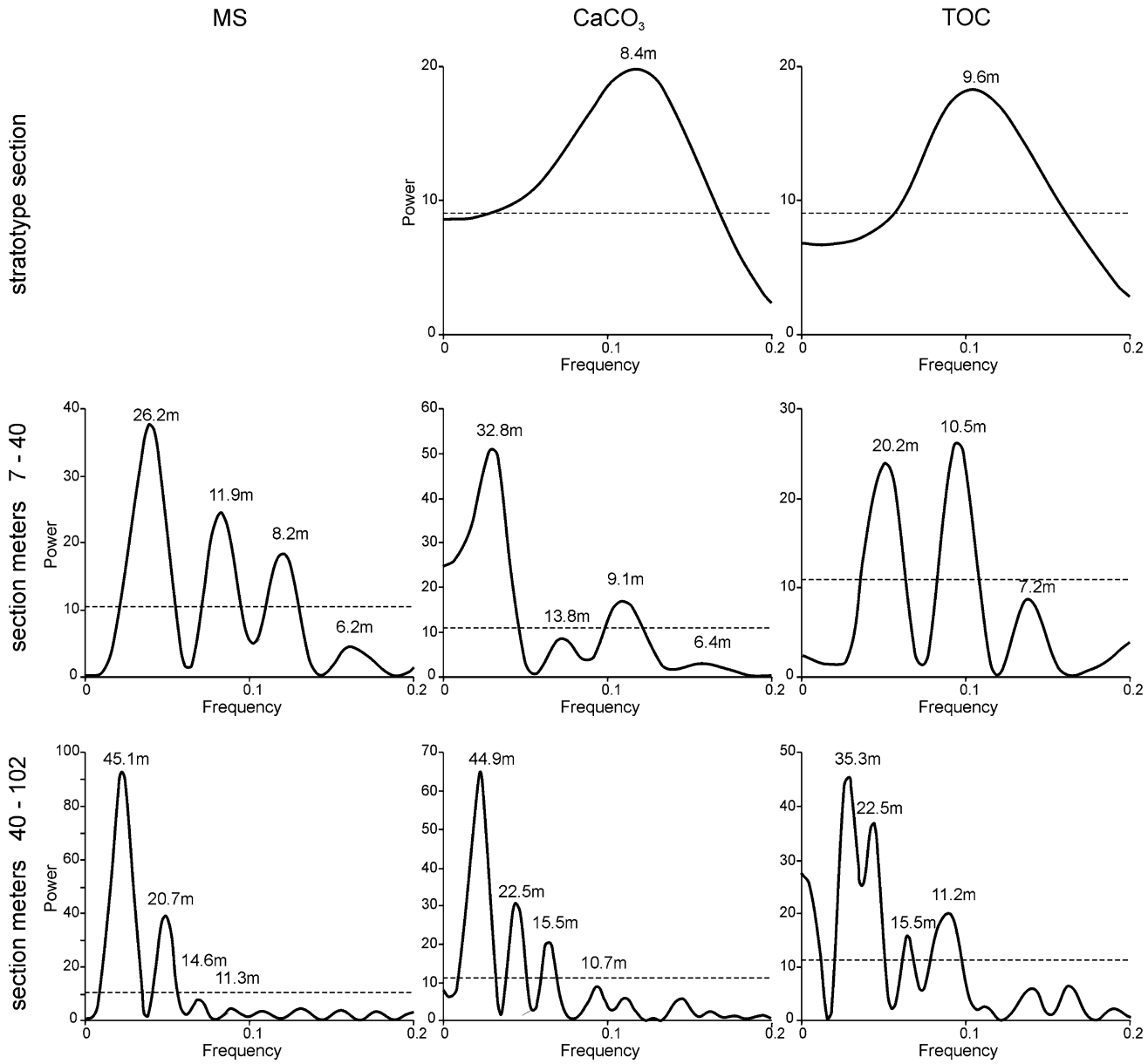

Fig. 3 Power spectra of magnetic susceptibility, calcium carbonate, and organic carbon in the three section parts (*dotted line* marks 1% error probability)

underestimation by the $^{40}Ar/^{39}Ar$ method (Kuiper et al. 2008). The tuff layer, from which the radiometric ages originate, is overlain by 52 m of siliciclastic fine-grained sediments still belonging to the Lower Lagenidae Zone, which is confirmed by the consistently abundant *Helicosphaera waltrans* and the planktonic foraminifer *Praeorbulina glomerosa glomerosa* (Hohenegger et al. 2009c).

The highest cross-correlation by far ($r = 0.2806$, $p_t = 3.61E\text{-}06$) marks the interval from −14.221 to −14.098 Ma (Fig. 4a). This correspondence is based on the rather parallel courses of insolation and MS.

From the remaining two significant correlations (Fig. 4a), the first ranging from −14.179 to −14.056 Ma is less significant than the correlation of the interval before, while the last and weak significant time interval from −13.898 to −13.775 Ma seems to be too young when adding the upper section part (110.4 kyr) and the overlying stratotype (17.7 kyr). Assuming a continuous succession of these three section parts without any break results in an upper limit of the stratotype section at −13.657 Ma, which is close to the NN5/NN6 boundary at −13.654 (Abels et al. 2005) falling at the end of the middle Badenian.

Therefore, the statistically best solution that is supported by radiometric, litho-, and biostratigraphic data certifies the time interval for the lower section core from −14.221 + 0.004/−0.005 Ma to −14.098 + 0.004/−0.005 Ma.

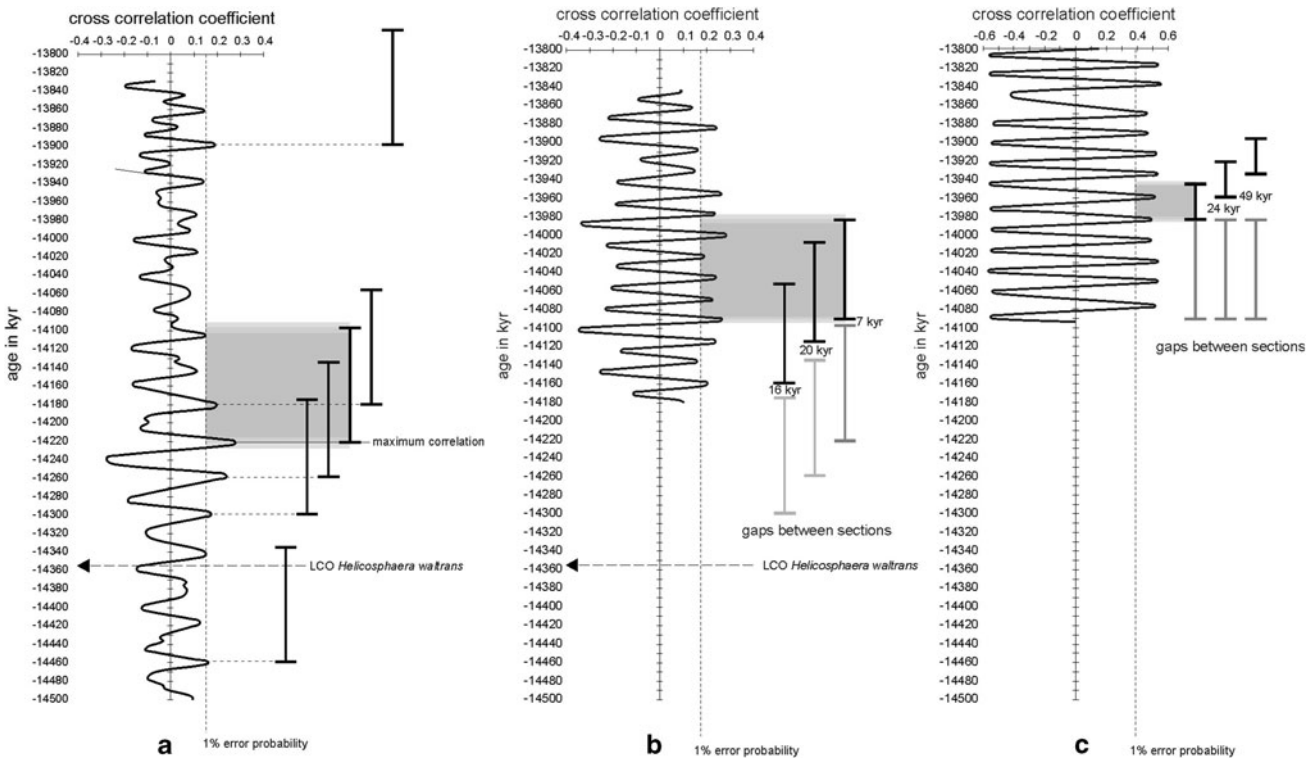

Fig. 4 **a** Lower part of drilled section; cross-correlation of MS and negative $CaCO_3$ with July insolation at 65° north. **b** Upper part of drilled section; cross-correlation of MS and negative $CaCO_3$ with July insolation at 65° north; the time gaps to earlier time determinations of the lower section are shown when using earlier significant intervals for the upper section. **c** Stratotype section; cross-correlation of negative $CaCO_3$ and organic carbon with July insolation at 65° north; the time gaps of later time determination to the upper section are shown. Different shading intensities characterize 1% confidence intervals

Dating the upper section part

A strong discontinuity in MS, $CaCO_3$, and C_{org} signals at 40-m section depth hints to a larger, tectonically caused disturbance (Fig. 2). Due to the strong differences between the uppermost lower section part and the lowermost upper section part, especially in organic carbon content, an overlap of both section parts must be excluded. After stretching the MS and (negative) $CaCO_3$ curves between 7 and 38.8 m, the resulting functions representing a time span of 110 kyr were again cross-correlated with the insolation curve starting in the uppermost part of the calibrated lower section at −14.180 Ma. Since the upper section is positioned above the lower section without overlapping, cross-correlation starts at −14.098 Ma (Fig. 4b). Due to the shorter time interval and tectonic disturbance, the correlations between insolation and MS/negative $CaCO_3$ are not as good as for the lower section. Nevertheless, the first significant interval ranges from −14.091 to −13.982 Ma, resulting in a mean gap of 7 kyr between both sections. The following 3 less significant intervals would mark larger gaps of 28, 52, and 74 kyr between both section parts, while the most significant peak in the studied interval would hint to a time gap of 97 kyr (Fig. 4b).

This indicates that the best solution is from −14.091 + 0.002/−0.003 Ma to −13.982 + 0.002/−0.003 Ma. The proposed time gap of 7 kyr is visible in the cutted cores by strong changes in the sediment type around 40.1 m (Wagreich et al. 2008).

Dating the stratotype section

After determining the time range of the cored section, the position of the stratotype section sampled in 1990 had to be checked along the timescale. Since no larger tectonic faults could be detected indicating a vertical displacement of the brickyard center, where the stratotype section was located (Papp and Steininger 1978), the stratotype section has to be correlated with the uppermost part of the cored section. Proofing coincidence, overlapping, or separation of both sections was done by cross-correlating the standardized content in $CaCO_3$ and organic carbon after logit transformation between both sections (Fig. 5a). The only significant correlation ($r = 0.827$, $n = 38$, $t_0 = 8.83$, $p(t_0) = 7.644\text{E-}11$) between the stratotype and the upper

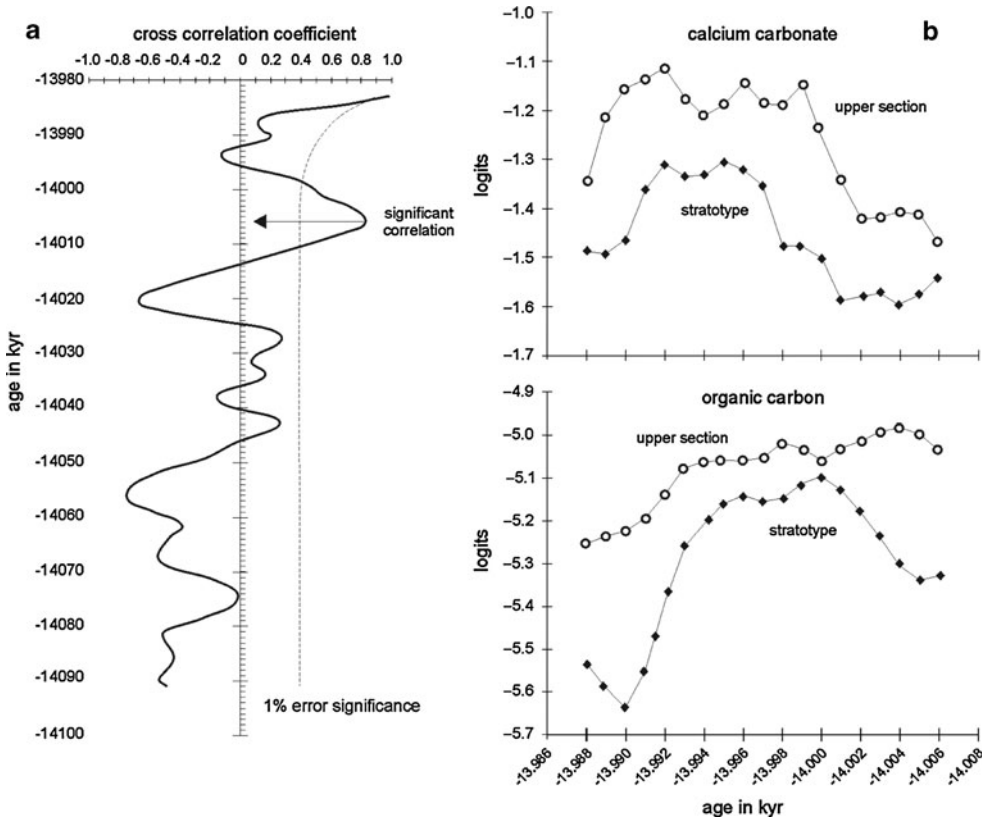

Fig. 5 **a** Cross-correlation of organic carbon and $CaCO_3$ between the stratotype section and the upper part of the drilled section. **b** The courses of $CaCO_3$ and organic carbon of the stratotype section and the upper part of the drilled section at the most significantly overlapping interval between −14.007 and −13.988 Ma (see Fig. 5a)

section part covers the interval between −14.006 and −13.988 Ma (Fig. 5a).

The main argument against this time calibration lies in the different position of their function courses, which are similar in both $CaCO_3$ and organic carbon (Fig. 5b). Similarities in the function forms were tested by linear correlation resulting in significant coincidence in both variables (Table 2), but the positions checked by paired *t* tests show significant differences in both geochemical characters (Table 2).

Consequently, the stratotype section was time calibrated continuing the cross-correlation between insolation and the measured physical and chemical variables. Organic carbon was now used in combination with the (negative) calcium carbonate content and compared with the insolation curve.

Cross-correlation of the stratotype section with insolation resulted in several highly significant peaks according to the short period (Fig. 4c). Starting with the end of the upper section part, this position shows the first significant correlation ($r = 0.496$, $n = 38$, $t_0 = 3{,}430$, $p(t_0) = 0.0008$) covering the interval from −13.982 to −13.964 Ma. This hints to a continuation of upper section part by the stratotype section without any gap (Fig. 4c), a geologically sound assumption.

The following three periods with similar significant cross-correlation show large gaps of 24, 49, and 70 kyr (Fig. 4c) that correspond to 11.4, 23.3, and 33.3 m distances above the uppermost cored section using the stratotype's sedimentation rate of 475 mm kyr^{-1}. Since the second solution with the second smallest time gap requires an unaccounted ∼13 m post-depositional down throw of the brickyard center in relation to the margin, the first solution of direct continuation must be accepted, which then corresponds much better to the structural geometry of the outcrop.

Therefore, the stratotype section of Baden/Sooss can be calibrated between −13.982 + 0.003/−0.002 Ma and −13.964 + 0.003/−0.002 Ma.

Discussion

The extremely significant cross-correlation between magnetic susceptibility combined with calcium carbonate on one hand and the July insolation curve at 65°N (Laskar et al. 2004) on the other hand allows to fix the base of the section cored near the Badenian stratotype at −14.221 + 0.004/−0.005 Ma, thus correcting the results obtained by Hohenegger et al. (2008, 2009a). Accepting the continuous transition from the upper drill section to the stratotype section, which is statistically supported, the complete section including the stratotype belonging to the regional Upper Lagenidae Zone, regarded as younger Early Badenian, finishes at −13.946 + 0.003/−0.002 Ma (Fig. 6).

Table 2 Testing the coincidence in calcium carbonate and organic carbon of the upper section part between −14.007 and −13.988 Ma (see Fig. 5) with the stratotype section by paired *t* test

Correlation of paired samples				
		n	Correlation	p(H_0)
$CaCO_3$	Upper section Stratotype	19	0.810	0.000
Organic carbon	Upper section Stratotype	19	0.814	0.000
Difference of paired samples				
		df	*T*	p(H_0)
$CaCO_3$	Upper section Stratotype	18	12.14	0.000
Organic carbon	Upper section Stratotype	18	7.87	0.000

Although the shapes of the curves are similar as tested by highly significant correlation, the difference between the curves is also highly significant

The proposed time calibration is also in accordance with an $^{40}Ar/^{39}Ar$ dating of −14.39 ± 0.12 Ma for the middle part of the Lower Lagenidae Zone (Handler et al. 2006), overlain by 53-m siltstones still belonging to the Lower Lagenidae Zone due to the presence of the nannoplankton *H. waltrans* and *Praeorbulina* (Hohenegger et al. 2009c).

Some problems but also solutions for the zonation of the Badenian arise by the proposed time calibration of the stratotype (Fig. 7). First, the Lower Lagenidae Zone should end with the LCO of *H. waltrans,* astronomically dated at −14.357 ± 0.004 Ma (Abdul Aziz et al. 2008). The next important biostratigraphic marker is the NN5/NN6 boundary dated by the LCO of *Sphenolithus heteromorphus* at −13.654 Ma (Abels et al. 2005), which was used as the Langhian/Seravallian boundary until the GSSP of the Seravallian was predated due to the strong $\delta^{18}O$ increase at −13.82 Ma found in the ocean record (e.g., Holbourn et al. 2005; Shevenell et al. 2004; Abels et al. 2005).

The presence of *S. heteromorphus* in the Badenian stratotype section (Rögl et al. 2008) and the lack of a

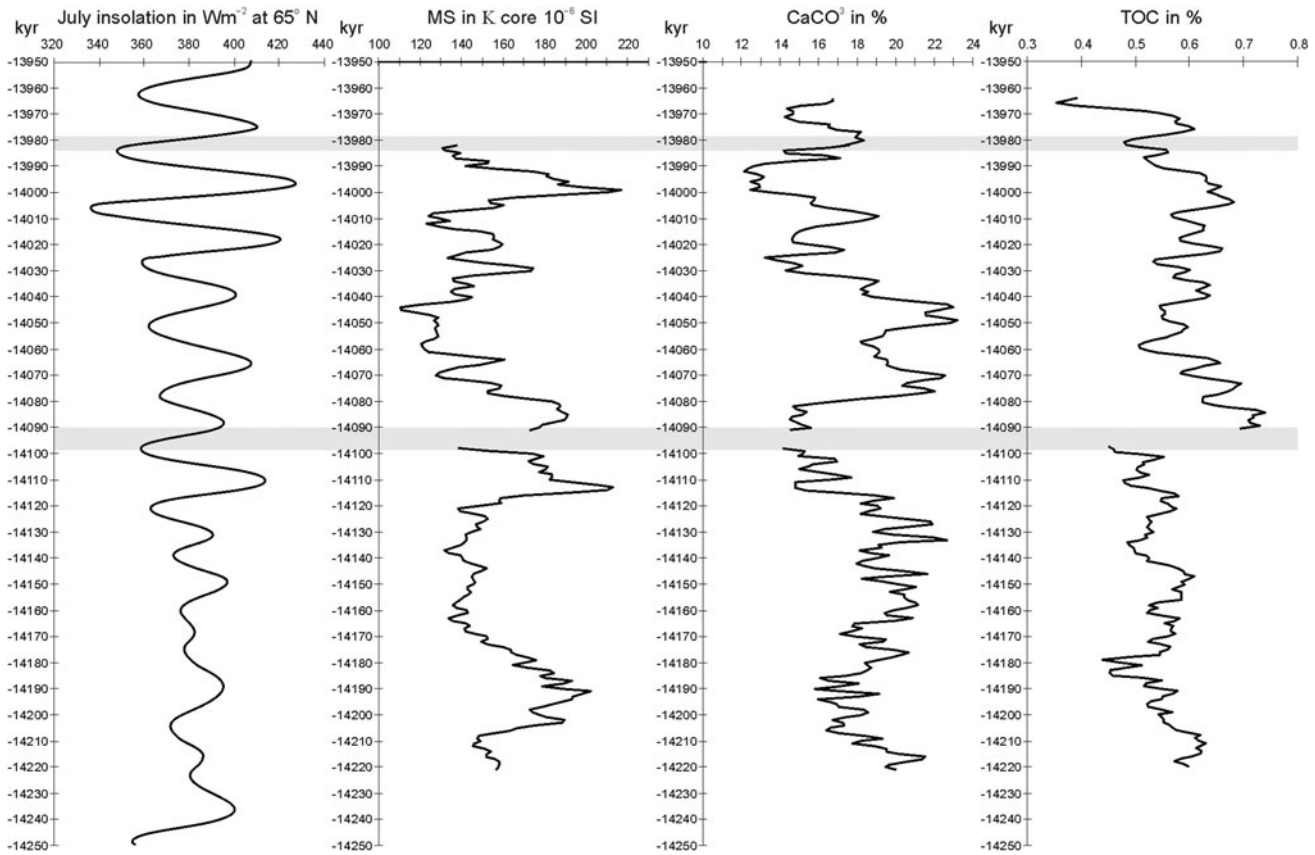

Fig. 6 Time calibrated courses of magnetic susceptibility, calcium carbonate, and organic carbon in the complete section compared with the July insolation at 65° north; *shaded areas* mark the proposed time gaps between section parts

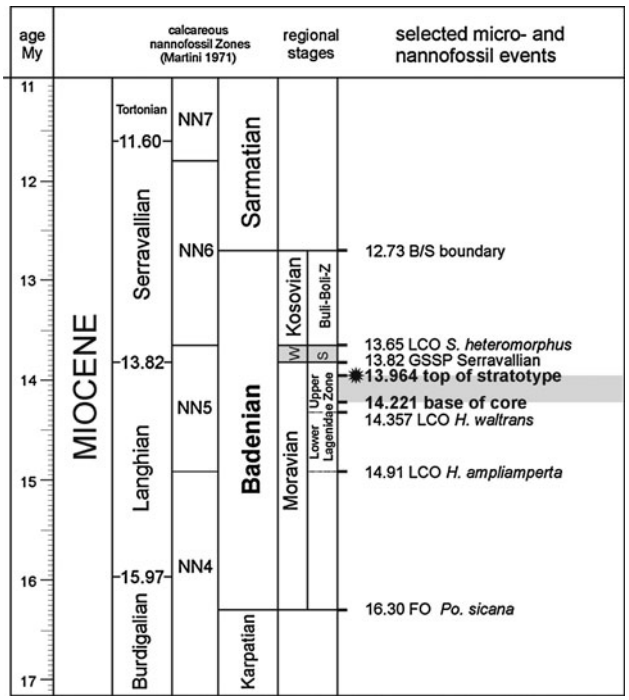

Fig. 7 Stratigraphic chart based on the timescale of Lourens et al. (2004) and Hohenegger et al. (2009a, b) showing the time span of Badenian substages

significant shift to higher $\delta^{18}O$ values in the complete section position the top of the Badenian stratotype section earlier than the Langhian/Seravallian boundary at −13.82 Ma, thus strengthening the time calibration of the stratotype's top at −13.946 + 0.003/−0.002 Ma.

By this time calibration, further problems arise in timing the boundaries between the Moravian (lower Badenian) and the Wielician (middle Badenian) substages (Papp and Steininger 1978; Piller et al. 2007). Taking the NN5/NN6 boundary at −13.654 Ma as the Wielician/Kosovian (=upper Badenian) boundary (e.g., Kováč et al. 2007; Strauss et al. 2006), then the Moravian/Wielician boundary must be placed between the top of the stratotype belonging to the Moravian at −13.946 Ma and the NN5/NN6 boundary. The most important global marker in this time interval is the significant $\delta^{18}O$ increase at −13.82 Ma marking the onset of the 'icehouse' phase during the middle Miocene (Holbourn et al. 2007). This prominent event is most probably expressed in the strong facies change as indicated by the sudden dominance of agglutinated foraminifera in the '*Spiroplectammina*' zone of the Vienna Basin (e.g., Rögl et al. 2008). Additionally, the GSSP of the Seravallian is positioned at this time point and thus also could be correlated with the Parathetys and used for the base of the Wielician (Piller et al. 2007).

Based on our results and accepting the NN5/NN6 boundary as the top of the Wielician, this substage must now be placed within the time interval from −13.82 to −13.654 Ma, thus covering only 166 kyr. The correct delimitation of the upper boundary and significance of such a short duration substage has to be checked by further analysis. In fact of such a short duration, a division of the Badenian into a Lower and an Upper Badenian may be preferable (see also Kováč et al. 2007), in contrast to the original definitions used by Papp and Steininger (1978).

Given the thick piles of sediments attributed to the middle Badenian (Wielician) elsewhere, especially thick evaporite deposits east of the Vienna Basin (e.g., Babel 2005; Peryt 2006), and the sequence stratigraphic framework by Harzhauser and Piller (2007), Kováč et al. (2004, 2007) and Strauss et al. (2006), we see a major misfit to the time frame with a strongly reduced duration of the middle Badenian based on our results from the Badenian stratotype. We therefore suggest that time correlations and chronostratigraphy within the Badenian are still biased. The picture of a consistent Badenian stratigraphy (e.g., Piller et al. 2007), including correlation of regional and local zones, sea-level evolution, and resulting sequence stratigraphy frameworks, has still major pitfalls, i.e., the middle Miocene "Wielician" salinity crisis in the Central Paratethys (Peryt 2006) may still fall well into the defined lower Badenian (i.e., Kováč et al. 2007). A concise chronostratigraphic system taking accurate and precise dating by orbital cyclicity for the whole stage has to be elaborated, which will then give undisputable correlations from the Paratethys into the global chronostratigraphy of the Miocene.

Conclusions

By combining outcrop and core data, it was possible to calibrate the Badenian stratotype by means of insolation cycles correlation to an age from −13.982 + 0.003/−0.002 Ma to −13.964 + 0.003/−0.002 Ma. This assigns an unexpected young, late Langhian age to the Badenian stratotype, although this interval is regarded still as lower Badenian in the Central Paratethyan chronostratigraphic framework. The age is high above the supposed base of the Badenian and thus indicates a rather long early Badenian in contrast to considerable shorter intervals of middle and late Badenian. This deviation is caused, among others, by the original definition of the early Badenian Lower Lagenidae Zone in the Vienna Basin, where the real range was underestimated compared with the extent of this zone in the Styrian Basin. Especially, the middle Badenian Wiecilian substage would then be reduced to a short interval. We conclude that the chronostratigraphy and sequence stratigraphy of the Badenian thus are still largely unsettled, and further time calibrations based on orbital cycles (like insolation) are needed to establish a precise and accurate time frame for the middle Miocene in the Paratethys.

Acknowledgments This work was supported by the Projects P13743-BIO, P13740-GEO, and P16793-B06 of the Austrian Science Fund (FWF). We thank Maksuda Khatun, Maria Meszar, and Silke Wagner for providing carbonate and organic carbon measurements, Anna Selge for making geomagnetic measurements, and Nils Anderson for analyzing stable isotopes. We also thank Katalin Bàldi, Stjepan Ćorić, Peter Pervesler, Fred Rögl, and Christian Rupp as coworkers in these projects. Especially, Fred Rögl was helpful in critically reading the manuscript and the reviewer Fabricio Lirer for his useful comments and critics. Additional thanks are due to Karl Rauscher and Herbert Summesberger for making available detailed sample sets of the gone Badenian stratotype.

References

Abdul Aziz H, Di Stefano A, Foresi LM, Hilgen FJ, Iaccarino SM, Kuiper KF, Lirer F, Salvatorini G, Turco E (2008) Integrated stratigraphy and $^{40}Ar/^{39}Ar$ chronology of early Middle Miocene sediments from DSDP Leg 42A, Site 372 (Western Mediterranean). Palaeogeogr Palaeoclimatol Palaeoecol 257:123–138

Abels HA, Hilgen FJ, Krijgsman W, Kruk W, Raffi I, Turco E, Zachriasse WJ (2005) Long-period orbital control on middle Miocene global cooling: integrated stratigraphy and astronomical tuning of the blue clay formation on Malta. Paleoceanogr 20:PA4012. doi:10.1020/2004PA001129

Babel M (2005) Event stratigraphy of the Badenian selenite evaporites (Middle Miocene) of the northern Carpathian Foredeep. Acta Geol Polonica 55:9–29

Batschelet E (1981) Circular statistics in biology. Academic Press, London

Bojar A-V, Hiden H, Fenninger A, Neubauer F (2004) Middle Miocene seasonal temperature changes in the Styrian basin, Austria, as recorded by the isotopic composition of pectinid and brachiopod shells. Palaeogeogr Palaeocimatol Palaeoecol 203:95–105

Cicha I, Papp A, Senes J, Steininger FF (1975) Badenian. In: Steininger FF, Nevesskaya LA (eds) Stratotypes of Mediterranean Neogene stages 2. VEDA, Bratislava, pp 43–49

Ćorić S, Hohenegger J (2008) Quantitative analyses of calcareous nannoplankton assemblages from the Baden-Sooss section (Middle Miocene of Vienna Basin, Austria). Geol Carpathica 59:447–460

Davis JC (2002) Statistics and data analysis in geology, 3rd edn. Wiley, New York

Hammer Ø, Harper DAT (2006) Paleontological data analysis. Blackwell, Malden, MA

Handler R, Ebner F, Neubauer F, Herman S, Bojar A-V (2006) $^{40}Ar/^{39}Ar$ dating of Miocene tuffs from Styrian part of the Pannonian Basin: an attempt to refine the basin stratigraphy. Geol Carpathica 57:483–494

Harzhauser M, Piller WE (2007) Benchmark data of a changing sea.—Palaeogeography, palaeobiogeography and events in the Central Paratethys during the Miocene. Palaeogeogr Palaeoclimatol Palaeoecol 253:8–31

Hohenegger J, Andersen N, Báldi K, Ćorić S, Pervesler P, Rupp C, Wagreich M (2008) Paleoenvironment of the Early Badenian (Middle Miocene) in the southern Vienna Basin (Austria)—multivariate analysis of the Baden-Sooss section. Geol Carpathica 59:461–487

Hohenegger J, Ćorić S, Khatun M, Pervesler P, Rögl F, Rupp C, Selge A, Uchmann A, Wagreich M (2009a) Cyclostratigraphic dating in the Lower Badenian (Middle Miocene) of the Vienna Basin (Austria): the Baden-Sooss core. Int J Earth Sci 98:915–930. doi:10.1007/s00531-007-0287-7

Hohenegger J, Pervesler P, Uchman A, Wagreich M (2009b) Upper bathyal trace fossils document palaeoclimate changes. Terra Nova 21:229–236

Hohenegger J, Rögl F, Ćorić S, Pervesler P, Lirer F, Roetzel R, Scholger R, Stingl K (2009c) The Styrian Basin: a key to the Middle Miocene (Badenian/Langhian) Central Paratethys transgressions. Austrian J Earth Sci 102:102–132

Holbourn A, Kuhnt W, Schulz M, Erlenkeuser H (2005) Impacts of orbital forcing and atmospheric carbon dioxide on Miocene ice-sheet expansion. Nature 438:183–487

Holbourn A, Kuhnt W, Schulz M, Flores J-A, Andersen N (2007) Orbitally-paced climate evolution during the middle Miocene "Monterey" carbon-isotope excursion. Earth Planet Sci Lett 261:534–550

Keferstein C (1828) Beobachtungen und Ansichten über die geognostischen Verhältnisse der nördlichen Klak-Alpenkette in Oesterreich und Baiern. Teutschland Geognostisch-Geol Dargestellt 5:1–425

Kocsis L, Vennemann VW, Hegner E, Fontignie D, Tütken T (2009) Constraints on Miocene oceanography and climate in the Western and Central Paratethys: O-, Sr-, and Nd-isotope compositions of marine fish and mammal remains. Palaeogeogr Palaeoclimatol Palaeoecol 271:117–129

Kováč M, Baráth I, Harzhauser M, Hlavatý I, Hudáčková N (2004) Miocene depositional system and sequence stratigraphy of the Vienna Basin. Cour Forsch-Inst Senckenberg 246:187–212

Kováč M, Andreyeva-Grigorovich A, Bajraktarevic Z, Brzobohaty R, Filipescu S, Fodor L, Harzhauser M, Nagymarosy A, Oszczypko N, Pavelic D, Rögl F, Saftic B, Sliva L, Studencka B (2007) Badenian evolution of the Central Paratethys Sea: paleogeography, climate and eustatic sea-level changes. Geol Carpathica 58:579–606

Kuiper KF, Deino A, Hilgen FJ, Krijgsman W, Renne PR, Wijbrans JRM (2008) Synchromizing rock glocks of earth history. Science 320:500–504

Laskar J, Robulet P, Joutel F, Gastineau M, Correia ACM, Levrard B (2004) A long-term numerical solution for the insolation quantities of the earth. Astron Astrophys 428:261–285

Linde A, Berchtold W (1976) Statistische Auswertung von Prozentzahlen. Birkhäuser, Basel

Lirer F, Harzhauser M, Pelosi N, Piller WE, Schmid HP, Sprovieri M (2009) Astronomically forced teleconnection between Paratethyan and Mediterranean sediments during the Middle and Late Miocene. Palaeogeogr Palaeoclimatol Palaeoecol 275:1–13

Lourens L, Hilgen F, Shackleton NJ, Laskar J, Wilson D (2004) The Neogene period. In: Gradstein FM, Ogg JG, Smith AG (eds) A geologic time scale 2004. Cambridge Univ Press, Cambridge, pp 409–440

Papp A, Steininger F (1978) Holostratotypus des Badenien. Holostratotypus: Baden-Sooss (südlich von Wien), Niederösterreich, Österreich. Badener Tegel—Keferstein, 1828 (Unterbaden; M4b; Obere Lagenidenzone). In: Papp A, Cicha I, Senes J, Steininger F (eds) M4 Badenien (Moravien, Wielicien, Kosovien). Chronostratigraphie und Neostratotypen Miozän der Zentralen Paratethys 6. VEDA SAV, Bratislava, pp 138–145

Papp A, Grill R, Janoschek R, Kapounek J, Kollmann K, Turnovsky K (1968) Zur Nomenklatur des Neogens in Österreich. Verh Geol Bundesanst 1968:9–27

Peryt TM (2006) The beginning, development and termination of the Middle Miocene Badenian salinity crisis in Central Paratethys. Sediment Geol 188–189:379–396

Piller WE, Harzhauser M, Mandic O (2007) Miocene Central Paratethys stratigraphy—current status and future directions. Stratigraphy 4:151–168

Popov SV, Rögl F, Rozanov AY, Steininger FF, Shcherba IG, Kovác M (eds) (2004) Lithological paleogeographic maps of

Paratethys. 10 Maps Late Eocene to Pliocene. Cour Forsch-Inst Senckenberg 250:1–46

Rögl F, Spezzaferri S, Coric S (2002) Micropaleontology and biostratigraphy of the Karpatian-Badenian transition (Early-Middle Miocene boundary) in Austria (Central Paratethys). Cour Forsch-Inst Senckenberg 237:47–67

Rögl F, Coric S, Harzhauser M, Jimenez-Moreno G, Kroh A, Schultz O, Wessely G, Zorn I (2008) The Middle Miocene Badenian stratotype at Baden-Sooss (Lower Austria). Geol Carpathica 59:367–374

Selge A (2005) Cyclostratigraphy by means of mineral magnetic parameters in the middle Badenian (Middle Miocene) core Sooß/Baden (Vienna Basin, Austria). Dipl Thesis Univ Leoben

Shevenell AE, Kennett JP, Lea DW (2004) Middle Miocene southern ocean cooling and antarctic cryosphere expansion. Science 305:1766–1770

Sprovieri M, Sacchi M, Rohling EJ (2003) Climatically influenced interactions. Paleoceanography 18:1034. doi:10.1029/2001PA000750

Strauss P, Harzhauser M, Hinsch R, Wagreich M (2006) Sequence stratigraphy in a classic pull-apart basin (Neogene, Vienna Basin). A 3D seismic based integrated approach. Geol Carpathica 57:185–197

Wagreich M, Pervesler P, Khatun M, Wimmer-Frey I, Scholger R (2008) Probing the underground at the Badenian type locality: geology and sedimentology of the Baden-Sooss section (Middle Miocene, Vienna Basin, Austria). Geol Carpathica 59:375–394